

## COMPARISON OF SOIL MOISTURE DATA FROM IN-SITU MEASUREMENTS WITH GEOLOGICAL DATA

Julian JAECKEL<sup>1,2</sup>, Marcin PAWLIK<sup>1,3</sup>, Bodo BERNSDORF<sup>1</sup>, Tobias RUDOLPH<sup>1</sup>

<sup>1</sup> Research Center of Post-Mining, Technische Hochschule Georg Agricola, Bochum, Germany

<sup>2</sup> Faculty of Geosciences, Ruhr University Bochum, Bochum, Germany

<sup>3</sup> Institute of Mine Surveying and Geodesy, Technical University Bergakademie Freiberg, Freiberg, Germany

### Abstract

As part of the MUSE project aimed at optimizing post-mining dewatering through multi-sensor geomonitoring, additional analyses were conducted based on soil samples. The aim of these analyses was to develop retention curves, which help determine critical soil physical parameters and soil moisture levels. Due to the absence of pressure pot analyses, grain size analysis was used to identify these critical parameters, allowing comparison with other data levels. In conclusion, the project results presented, that the methods used demonstrated a high degree of consistency with official soil data (maps and tables) in the working area, making them suitable for future studies on soil moisture, potentially eliminating the need for time-consuming laboratory analyses. The Soil Map 1:50,000 (BK50) data can serve as a benchmark for estimating soil moisture values in large-scale investigations.

Keywords: soil moisture, water content, field capacity (FC), permanent wilting point (PWP)

## 1. INTRODUCTION

The coal mining industry has significantly shaped the Ruhr area. Since the beginning of the 19th century, coal production in Germany increased. Over time, new technologies and processes made it possible to mine deeper seams in northern areas. Starting in 1958, several factors led to the coal crisis across Europe, which also affected the Ruhr area [1]. This led to a decline in the amount of hard coal produced. As a result of the fact that German coal mining was no longer competitive, the Prosper-Haniel mine in Bottrop, the last in Germany, closed in December 2018 [2].

The project "MUSE – Multisensor Geomonitoring for Optimizing Post-Mining Water Management" focuses the monitoring and management of regions impacted by mining activities. These areas, known as polders, have significantly subsided due to mining activities. In Figure 1, the MUSE project area is outlined in blue and is influenced by the former Prosper-Haniel mine. The aim of the

---

<sup>1</sup> Corresponding author: JULIAN JAECKEL, Technische Hochschule Georg Agricola, Research Center of Post-Mining, Herner Straße 45, 44787 Bochum, Germany, [Julian.Jaeckel@thga.de](mailto:Julian.Jaeckel@thga.de)

following study is to analyse and classify soil samples taken in 2022 and to compare them with soil data from Geological Survey Authority available for the area. The comparison is conducted using retention curves, which represent pore size distribution and allow for the derivation of the soil's water retention properties [3]. This is referred to below as the pF curve, which can be derived from various soil properties, such as hydraulic characteristic, morphological and chemical features, and grain size distribution [4]. The pF curves can be used to read the field capacity (FC) and permanent wilting point (PWP). Both are soil parameters that determine water content under defined conditions. Within a pF curve, the values FC can be read at 1.8 and PWP values at 4.2.

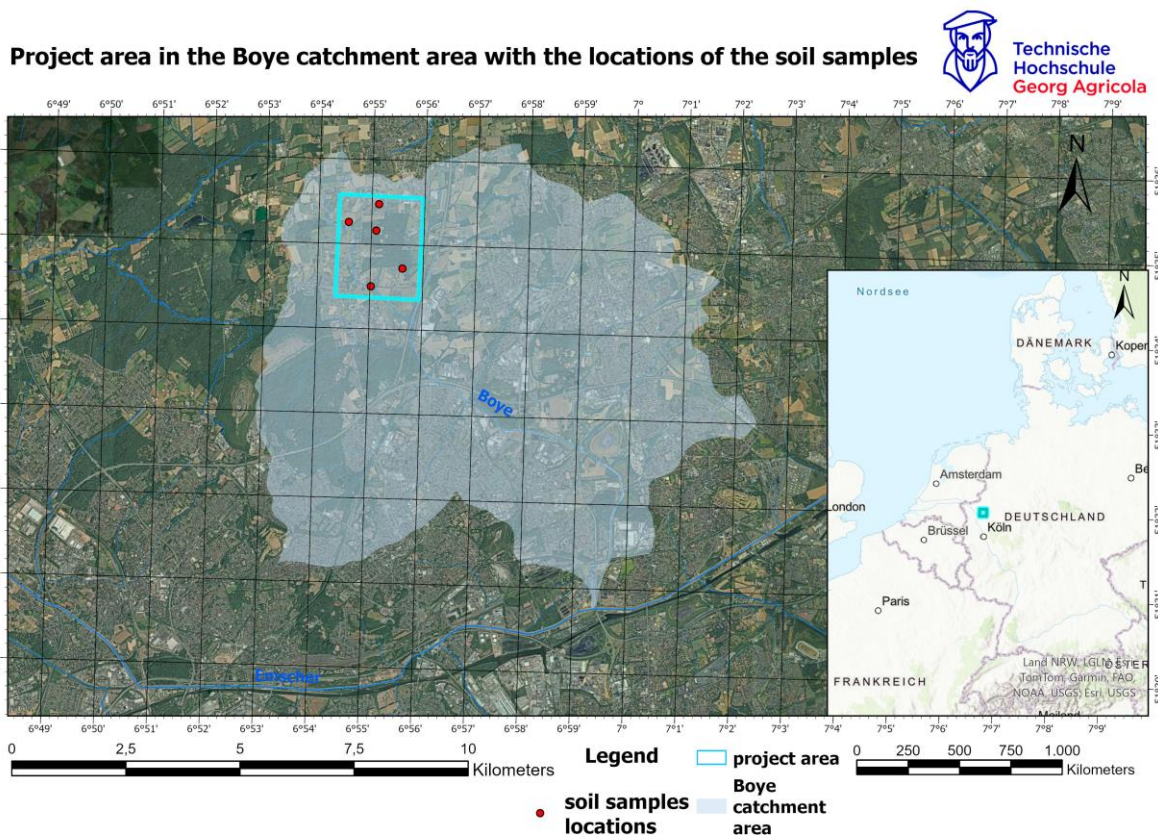


Fig. 1. Locations of soil samples. Sources of base map: [5,6]

Soil moisture can be measured using three methods: in-situ sensors, laboratory drying, or remote sensing methods. In-situ and laboratory measurements are significantly more precise, focusing on smaller areas, whereas the less accurate remote sensing can cover larger areas [7,8]. A commonly used in-situ sensor measurement method is Time-Domain Reflectometry (TDR). TDR is based on the principle that the dielectric constant of moisture/water is higher than that of mineral soil. The sensors measure the signal length along probe rods, and this signal travel time is used to determine the water content [9]. TDR in-situ sensors were also installed at the sample sites taken. Abbes et al. [7] and Yu et al. [10], among others, have addressed soil moisture measurement, though they relied on remote sensing methods rather than deriving from soil samples using in-situ sensor technology. In addition to Abbes et al., Bauer-Marschallinger et al. [7,8] also dealt with soil moisture measurement via remote sensing, specifically using radar satellites such as Sentinel-1A, transmit waves to the earth in the form of microwaves. By the reflection of these waves provides data about the Earth's surface, which can be

analyzed using a specific geophysical computational model to calculate soil moisture values [8]. It is clear from Abbes et al. [7] and Bauer-Marschallinger et al. [8] that climate change can be better understood by observing soil moisture. One way to determine soil moisture-related factors in the laboratory is by using pressure pots. In this method, a fully saturated soil sample is drained at different pressure levels using fine-pored ceramics and atmospheric pressure. The water content is then determined by weighing. However, this method requires a laboratory equipped with the necessary tools and is time-intensive. In Schelle et al. [11], soils from Germany were sampled using the pressure plate method, as well as three other laboratory methods, each requiring specific laboratory equipment.

This paper describes a self-developed and alternative project that attempts to determine soil moisture without having to carry out a more complex laboratory analysis. In contrast to the methods described in Schelle et al. [11] it is carried out by means on a grain size analysis. This eliminates the need for additional materials to determine soil moisture beyond those used in particle size analysis. Additionally, it is possible to use disturbed samples, as particle size analysis does not depend on whether samples are disturbed or undisturbed. This laboratory investigation and the attempt to determine soil moisture through using the grain size analysis were conducted.

The area is part of the Boye catchment area. Figure 1 shows the catchment area of the Boye and the project area can be recognised within the catchment area with the locations where the soil samples were taken. The aim of this article is to show how the MUSE project proceeded in order to find a way to check self-collected soil samples for official geological data.

## 2. METHODOLOGY

As part of the MUSE project, soil samples were taken in 2022, which now form the basis for the following research. The aim of this article is to show how the MUSE project proceeded in order to find a way to check self-collected soil samples for official geological data. This is attempted with the help of retention curves.

The methodology of research (Figure 2) begins with soil sampling, which involves collecting soil profiles from various locations for further laboratory analysis. Subsequently, the samples undergo soil classification, where they are categorized based on their physical and chemical properties. Following this, the soil analysis using retention curves (pF) is performed, employing templates from the textbook by Scheffer/Schachtschabel (Figure 3) [12], to identify critical soil-physical parameters such as field capacity and permanent wilting points. These retention curves provide a means to determine volumetric soil moisture values. The derived parameters are then compared with BK 50 geological data, integrating grain size analysis results due to the absence of pressure pot measurements. Finally, an assessment of soil moisture estimation methods is conducted to evaluate the compatibility between self-collected data and official geological datasets. This systematic approach ensures the integration and validation of soil properties across different data sources.

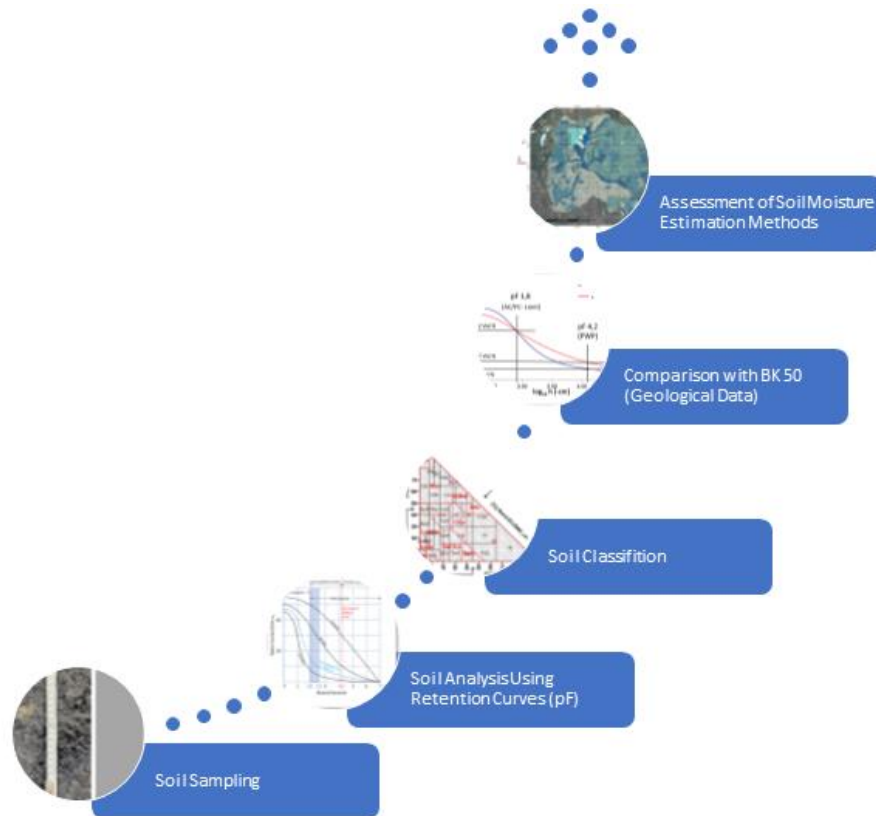


Fig. 2. Methodology of research

Figure 3 shows the estimation of the position of the soil analyses in such a curve before the analyses (blue dashed line) and the correct calculation of the retention curves in the working area. The diagram illustrates the soil water retention curve, showing the relationship between soil matric potential (expressed in pF) and soil water content (in volumetric percentage). The chart includes three distinct curves representing different soil types: sandy soils, silt soils, and clay soils. Sandy soils have the lowest water retention capacity and a steeply declining curve, silt soils are intermediate, while clay soils exhibit the highest water retention capacity and a more gradual curve.

Several key points are highlighted on the graph. The field capacity represents the range of matric potential (approximately 1.8–2.5 pF) where the soil retains the maximum amount of water in its capillary pores that is still available to plants. The area to the left of this point is referred to as air capacity, indicating water that drains quickly from the soil due to gravity. The permanent wilting point, marked by a red line at 4.2 pF, is the minimum soil water content at which plants can no longer extract water, leading to wilting. The area between the field capacity and the permanent wilting point is known as plant-available soil water, representing the range of water that plants can effectively utilize. Beyond the permanent wilting point, the water is classified as not plant-available, as it is held too tightly by the soil particles for plants to access.

Additionally, the graph highlights the soil's working area, shown with blue shading, which represents the range of matric potential where the soil is suitable for cultivation. The diagram illustrates the differences in the water storage and availability capacities of various soil types. Clay soils retain

larger amounts of water, but a significant portion of it is unavailable to plants, while sandy soils have lower water retention but release it more readily. This chart emphasizes the varying water management characteristics of different soil types.

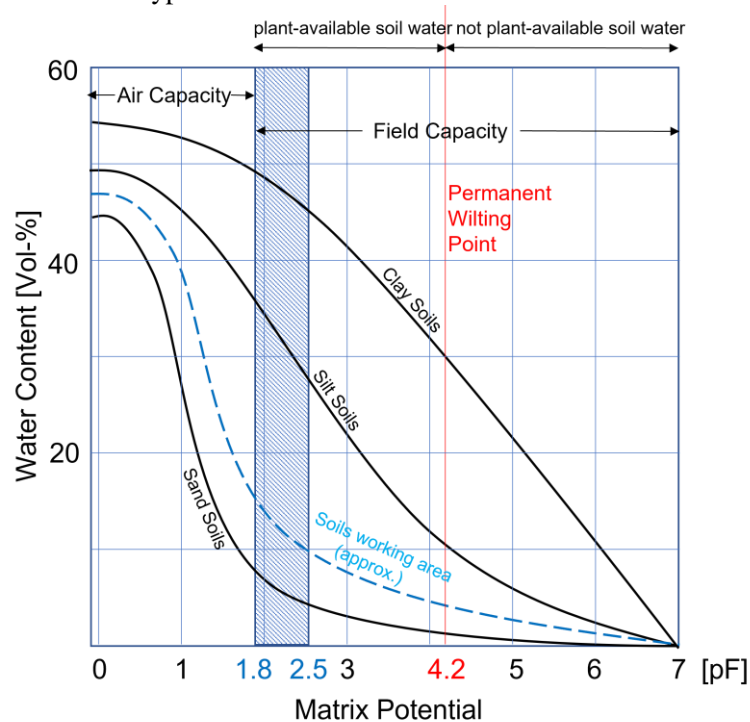


Fig. 3. Template of pf-curves. Source: modified from [12]

First the samples were separated, stored and dried. This was followed by a particle size analysis, which was only carried out in accordance with the DIN ISO 11277:2020-04 [13] or DIN ISO 11277:2002-08 [14] standard. This step was deliberately chosen as the ecologically effective landscape features were to be evaluated and not the “quartz content” determined. As a result, humus, lime or other concretions were not destroyed in advance during sample preparation. However, the humus content was determined as a percentage. This grain size analysis was used to classify the soil types.

The focus was deliberately placed on USDA soil classes (soil classes according to the US Department of Agriculture), as only 12 soil types are involved and not the significantly higher and finer subdivision of KA5 (soil classes according to the ger. Kartieranleitung 5 - Soil mapping guide) [15]. There are published conversion options for the USDA classes, from which pF curves can be derived based on grain size analyses [18]. The Geological Survey of North-Rhine Westphalia’s website offers a calculator that determines the corresponding soil type based on grain size analysis [16]. As a final classification of soil classes, the classification of the Food and Agriculture Organization of the United Nations (FOA) was used, which, like the USDA, is based on the same 12 soil classes [15]. The results revealed that, according to this classification, only two distinct soil types are present across the entire “MUSE” study area, based on the analysis of all collected soil samples. These were sandy loam and loamy sand. In the German KA5, this corresponds to the areas of strong loamy sands, loamy sands, sandy silts and sands [15].



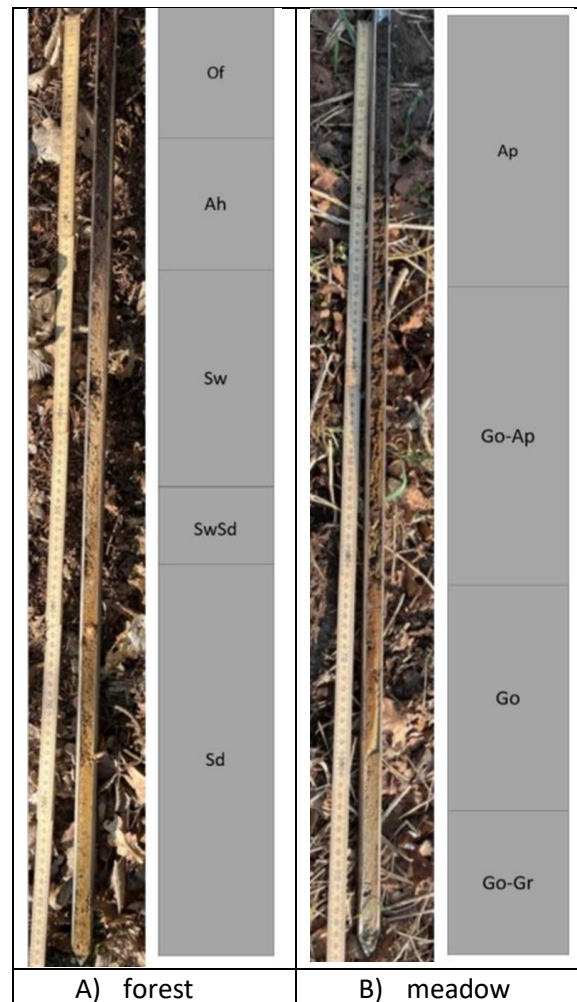


Fig. 5. Soil sampling from A) forest area and B) meadow area.

The example profiles (Figure 5) show two common soil types and the related soil water dynamics. In forested areas Stagnosols (German Term: Pseudogley) are widely distributed because a dense (clay) layer prevents precipitation to flow to the ground water layer immediately. The dense layer is marked as Sd in Figure 5. It reduces the speed of water flow. This can be easily observed in the Sw-Layer above where the precipitation is stowed. Thus, it stays wet for a longer time. This layer shows streaks and concretions of dissolved and re-precipitated manganese and iron. Due to the fact that this is difficult for agriculture (heavy machines) such sites are usually shows forest as land use category. In between the both layers one can observe somewhat like a transition layer (SwSd). This layer is not typical for a natural grown soil. It indicates anthropogenic influence, in the case of the study area it can be related to the subsidence and following drainage of the region [12].

The same is true for the right profile of Figure 5. This picture shows a Gleysol, for which the common land use is grassland utilization. Geographically meadow plots laying closer to the brooks and the soil water dynamic is influenced by ground water. Typical profile shows a humic layer on top but because the grassland utilization is an agriculture utilization the plots was plough and thus, shows an Ap horizon (p for ploughing). Below that in classic profiles the Go horizon follow. G stands for ground

water, o for oxidized. This horizon looks very like the Sw horizon of the Stagnosol but the water comes from below – groundwater instead of precipitation. It is the change of ground water levels which is reflected wet and dry phases over the year. It also shows streaks and concretions of dissolved and re-precipitated manganese and iron. The Gr-Layer is usually pale grey because it is affected by groundwater most time of the year which caused reductive conditions (the “r” in Gr) in this horizon. Like in the Stagnosol the Gleysols in this area are anthropogenic affected. That is the reason why we find transition layers as well in the Gleysols due to subsidence with a change of groundwater level and subsequent drainage which brings the soil back close to natural conditions [12].

For six of such profiles, weather stations with soil moisture sensors were installed at several depths (5 cm, 30 cm, 60 cm). This provided the advantage of observing and analyzing the soil profile directly and over a larger area and in terms of its soil water dynamics. The soil samples were collected using sampling cylinders. In comparison to the borehole analysis some more parameters were determined for the stations, as the cylinder samples were further analyzed in the laboratory, for example, to determine the humic content and perform grain size analysis. Samples were collected at the level of the sensors, as well as at depths corresponding to the foundations of the localizations (5 cm, 30 cm, and 60 cm).

Since only a grain size analysis and the determination of the soil types were available, so-called “lookup tables” were used. These specify the hydrological parameters for soil types. In this case, lookup table 19 from the literature by Toth et al. [18] was used. There were two main reasons for this. Firstly, this lookup table gave the hydrological parameters in USDA soil classes (not available for the soil type groups of KA5), and secondly, these parameters were determined from Western European soils [18]. The hydrological parameters used were now evaluated in an Excel diagram provided. This diagram can also plot a pF curve. In addition, the field capacity (FC), the permanent wilting point (PWP) and the plant-available water are indicated (Figure 6). Both the FC and the PWP are clearly definable and lie at pF 1.8 (air/field capacity limit) and pF 4.2 (PWP) [12].

The Figure 6 illustrates the water retention curves for two soil types: loamy sand and sandy loam. The vertical axis represents water content in the soil (expressed in  $\text{cm}^3$  of water per  $\text{cm}^3$  of soil), while the horizontal axis shows the logarithm ( $\log_{10}$ ) of the soil water suction (h) in centimetres, which corresponds to the soil matric potential (pF). The key points on the graph are the pF 1.8 threshold, corresponding to the field capacity (FC), and the pF 4.2 threshold, representing the permanent wilting point (PWP). Field capacity (pF 1.8) is the state at which the soil holds the maximum amount of water available to plants after gravitational water has drained. The graph shows that sandy loam retains more water at this threshold compared to loamy sand. The permanent wilting point (pF 4.2) is the minimum water content at which plants can no longer extract water, leading to wilting. Loamy sand has a lower water content at this point compared to sandy loam. For loamy sand, the water content at pF 1.8 is approximately  $0.32 \text{ cm}^3/\text{cm}^3$ , decreasing to about  $0.09 \text{ cm}^3/\text{cm}^3$  at pF 4.2. For sandy loam, the water content at pF 1.8 is about  $0.40 \text{ cm}^3/\text{cm}^3$ , dropping to around  $0.12 \text{ cm}^3/\text{cm}^3$  at pF 4.2. The graph demonstrates that sandy loam retains more water at both the field capacity and the permanent wilting point, making it richer in plant-available water compared to loamy sand. This information is crucial for soil water management, agricultural planning, and efficient use of irrigation systems.

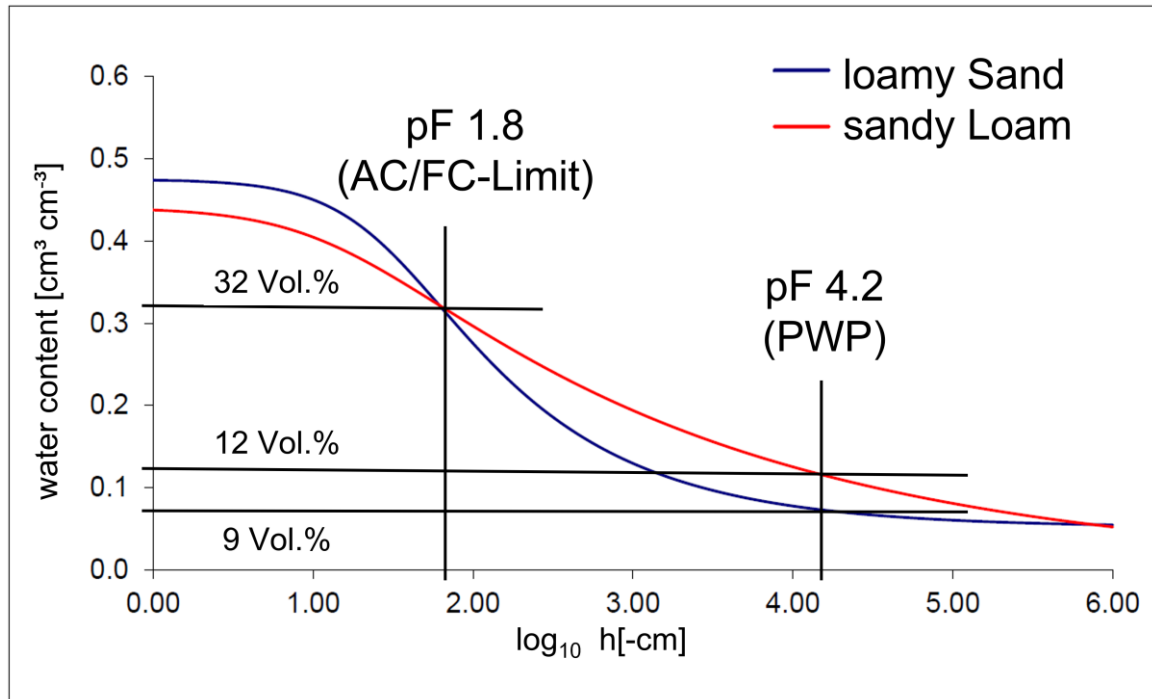


Fig. 6. Comparison of the pF curves in the working area with drawing of the important limit's pF 1.8 an pF 4.2.  
Source after [12]

Since the grain size distribution, the soil types, the field capacity and the permanent wilting point were determined during the implementation, the next step is to compare the data with the official data of the Geological Survey of North-Rhine-Westphalia (Figure 7). The map shows the distribution of soil water content at the permanent wilting point (PWP), expressed in volumetric percentages (%), across the studied area. The analysis covers both the topsoil layer (up to 10 cm depth) and the entire soil profile. The data were provided by the Geological Service NRW (BK50) as part of research. Calculations were based on reference depth, field capacity, and plant-available water capacity. The map uses different shades of blue to represent the soil water content at the permanent wilting point. Lighter shades indicate lower water content ( $\leq 5\%$ ), while darker shades represent higher water content ( $>12\%$ ). Additionally, the map highlights a specific project catchment area outlined in red for detailed investigation.

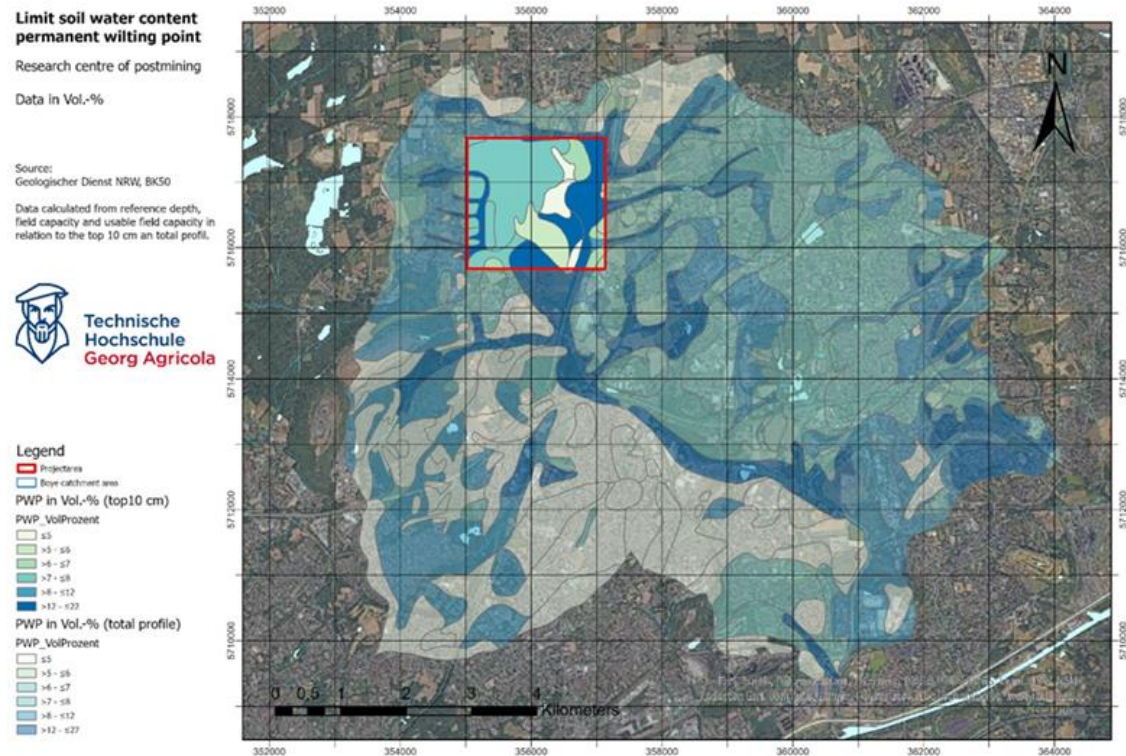


Fig. 7. Limit soil water content at the PWP in the Boye catchment area. Source of base map: [5]

For this purpose, the soil map 1:50.000 (ger. Bodenkarte 50 - BK50) from 2014 with its individual data/layers was downloaded from the NRW Geological Survey. The root zone, defined as the portion of the soil where plant roots actively grow and extract water and nutrients, typically extends to varying depths depending on soil type and vegetation. Because the standard BK50 data represents an average value over the entire root zone, the values for 1dm (10cm), 3dm (30cm) and 6dm (60cm) had to be extracted and used separately with the help of additional American standard code for information interchange (ASCII) data supplied [19]. This data corresponds to the depths of the soil samples taken and the soil sensors installed. The data was assigned to the respective soil units using the ArcGIS software via Join and three data sets were created, each representing the Boye catchment area, the BK50 and the data for the corresponding depth. Because the BK50 does not contain any values for the permanent wilting point this was also calculated from the specified values for field capacity and available water capacity [15] (Formula 3.1):

$$PWP = \frac{FC}{M} - \frac{AWC}{M} \quad (3.1)$$

Where:

PWP = Permanent wilting point in vol. % water content  
 FC = Field capacity in vol. % water content  
 AWC = available water capacity in vol. % water content  
 M = Thickness of the horizon in dm

The soil analysis was conducted using samples collected from five stations. Each station provided three samples taken at depths of 5 cm, 30 cm, and 60 cm, resulting in a total of 15 samples. The soil types derived from these samples were compared with the soil types identified in the BK50 dataset. The comparison revealed a 73% agreement between the soil types determined from the station samples and those obtained from the BK50 dataset. At each station, the soil types varied slightly depending on the depth of sampling. For example, at 5 cm, the soil types generally consisted of sandy loam, while at 30 cm and 60 cm, transitions to clay loam or silty clay were observed at certain stations. These variations highlight the heterogeneity of soil composition within the region. The agreement with the BK50 dataset was generally consistent, but minor discrepancies occurred in some cases, particularly at deeper layers, likely due to local soil heterogeneity or differences in classification methods and sample resolutions. Each sample point was characterized by its station ID, depth, and the soil type identified. For instance, Station 1 at 5 cm depth indicated sandy loam, at 30 cm depth showed silty loam, and at 60 cm depth transitioned to silty clay. Similar patterns were observed at other stations, where surface layers were often dominated by sandier textures, and deeper layers contained more clay or silt. The spatial distribution of soil types across the stations showed notable consistency in surface layers, but variability increased with depth. This suggests that the geological and environmental processes influencing soil development in the area have a more significant impact at deeper layers.

In summary, the soil analysis provided a detailed understanding of the soil composition at different depths across the stations. The 73% agreement with the BK50 data validates the findings while highlighting some localized differences that require further investigation. These results are crucial for understanding soil properties, including water retention and permeability, which have implications for land management and reclamation in the study area. The values of the field capacity and the permanent wilting point were compared in the same way. Furthermore, deviations of the different soil types are similar in both the self-collected and the Geological Survey data. This was to be expected, as the own grain size analyses were only processed in accordance with DIN [13,14]. It should also be noted that not every soil type has a dedicated field capacity or a dedicated permanent wilting point. Certain bandwidths must also be taken into account here. The ranges of field capacity and permanent wilting point can be seen in each soil type from to. It is therefore not given that each soil type has an exact value of field capacity or permanent wilting point.

#### 4. CONCLUSIONS

Although the analysis was only based on the DIN standard [13,14], there is a high degree of agreement both for the soil types and for the critical soil physical parameters. This means that the plausibility of the Geological Survey's soil maps can be assessed with sufficient accuracy as usable for large-scale analyses and is therefore recommended. BK 50 can therefore be used in future when extrapolating the methods applied with regard to the data integration of in situ data. The assessment of the in-situ measurements can also be compared directly with the ground data of the Geological Survey simply due to the measurement inaccuracies of the sensors. This means that - maybe not in general but at least for the working area - time-consuming laboratory analyses will no longer be necessary in future and the BK 50 can be used as a benchmark for estimating soil moisture values from Sentinel 1 data, for example, in the case of large-scale investigations.

It should be noted that the BK50 soil map is provided by the state of North Rhine-Westphalia. It provides the BK50 only for the federal state of NRW. Other federal states also provide soil maps in the BK50 format [20]. There was no comparison made with other German federal states. This poses the problem that no statement can currently be made for the whole of Germany.

Additionally, the limited number of soil samples may not fully capture the spatial variability of soil properties within the study area. The study was based on one-time sampling and analysis, which did not account for temporal changes in soil moisture potentially influenced by seasonal or climatic variations. While the study highlights a 73% agreement between soil types determined through particle size analysis and those represented in the BK50 map, the lack of detail in the methodology regarding the statistical methods used weakens the robustness of the comparative analysis. Furthermore, comparisons with data from public databases would be necessary to strengthen the reliability and broader applicability of the findings. Although the paper evaluates the effectiveness of the proposed method and its potential applications, it should also acknowledge these limitations.

### ADDITIONAL INFORMATION

Thanks are due to PD Dr. Lutz Weihermüller, who was instrumental in creating the pF curves. The MUSE project – Multisensor Geomonitoring for Optimizing Post-Mining Water Management – is funded by RAG Stiftung (No. 2021-0002).

### REFERENCES

1. Bundeszentrale für politische Bildung 2019. Der Ruhrbergbau. Von der Industrialisierung bis zur Kohlenkrise [The Ruhr mining industry. From industrialisation to the coal crisis]. <https://www.bpb.de/shop/zeitschriften/apuz/283262/der-ruhrbergbau/> (last accessed 04 November 2024).
2. Witsch, K 2018. Ein letztes „Glück auf!“ – Mit der Steinkohle endet für Deutschland eine Ära. [One last ‘Glück auf!’ - An era ended for Germany with hard coal]. <https://www.welt.de/politik/deutschland/article185986296/Zechenschliessung-Ein-letztes-Glueckauf-fuer-den-Bergbau.html> (last accessed 04 November 2024).
3. Spektrum 2000. Saugspannungskurve. [Suction stress curve]. <https://www.spektrum.de/lexikon/geowissenschaften/saugspannungskurve/14071> (last accessed 04 November 2024).
4. Weihermüller, L, Lehman, P, Herbst, M, Rahmati, M, Verhoef, A, Or, D, Jacques, D and Vereecken, H 2021. Choice of Pedotransfer Functions Matters when Simulating Soil Water Balance Fluxes. *Journal of Advances in Modeling Earth Systems* **13**, 1-30.
5. ESRI 2024. ArcGIS Pro 3.2.1 (last accessed 04 November 2024).
6. Landesamt für Natur, Umwelt und Verbraucherschutz Nordrhein-Westfalen 2024. Gewässerstationierungskarte des Landes Nordrhein-Westfalen. [Waterway stationing map of the state of North Rhine-Westphalia]. <https://www.lanuv.nrw.de/umwelt/wasser/oberflaechengewaeserfluesse-und-seen/fliessgewaeser/gewaesser-stationierungskarte/> (last accessed 11 November 2024).
7. Abbes, AB, Jarray, N and Farah, IR 2024. Advances in remote sensing based soil moisture retrieval: applications, techniques, scales and challenges for combining machine learning and physical models. *Artificial Intelligence Review* **57**, **224**, 1-22.
8. Bauer-Marschallinger, B, Naeimi, V and Wagner, W 2015. Bodenfeuchtemessung durch Radarsatelliten: Aktuelle Entwicklungen zur Erfassung auf lokaler Ebene [Soil moisture measurement by radar satellites: Current developments for localised detection]. *Österreichische Wasser- und Abfallwirtschaft* **67**, 422–431.

9. UMEG Zentrum für Umweltmessungen, Umwelterhebungen und Gerätesicherheit Baden-Württemberg 2002. Bodenfeuchtemessung [Soil moisture measurement]. <https://pudi.lubw.de/detailseite/-/publication/63911> (last accessed 04 November 2024).
10. Yu, L, Gao, W, Shamshiri, RR, Tao, S, Ren, Y, Zhang, Y and Su, G 2021. Review of research progress on soil moisture sensor technology. *International Journal of Agricultural and Biological Engineering* **14(4)**, 32–42.
11. Schelle, H, Heise, L, Jänicke, K and Durner, W 2013. *Wasserretentionseigenschaften von Böden über den gesamten Feuchtebereich – ein Methodenvergleich [Water retention properties of soils over the entire moisture range - a comparison of methods]*. Proceedings of 15. Gumpensteiner Lysimetertagung, Gumpenstein, Austria, April 16-17, 213-216.
12. Amelung, W, Blume, H-P, Fleige, H, Horn, R, Kandeler, E, Kögel-Knaber, I, Kretschmar, R, Stahr, K and Wilke, B-M 2018. *Scheffer/Schachtschabel – Lehrbuch der Bodenkunde 17. Aufl. [Scheffer/Schachtschabel - Textbook of Soil Science 17th ed]*. Heidelberg: Springer Spektrum.
13. DIN ISO 11277:2020-04 2020. Bodenbeschaffenheit - Bestimmung der Partikelgrößenverteilung in Mineralböden - Verfahren mittels Sieben und Sedimentation [Soil properties - Determination of particle size distribution in mineral soils - Method using sieving and sedimentation]. <https://www.dinmedia.de/de/norm/iso-11277/324323392> (last accessed 04 November 2024).
14. DIN ISO 11277:2002-08 2002. Bodenbeschaffenheit - Bestimmung der Partikelgrößenverteilung in Mineralböden - Verfahren mittels Siebung und Sedimentation [Soil properties - Determination of particle size distribution in mineral soils - Method using sieving and sedimentation]. <https://www.dinmedia.de/de/norm/din-iso-11277/53934894> (last accessed 04 November 2024).
15. Bundesanstalt für Geowissenschaften und Rohstoffe 2008. Die bodenspezifischen Kennwerte der KA5 [The soil-specific characteristic values of the KA5]. [https://www.bgr.bund.de/DE/Themen/Boden/Netzwerke/AGBoden/Downloads/KA5\\_bodenspezKennwerte.pdf?\\_\\_blob=publicationFile&v=2](https://www.bgr.bund.de/DE/Themen/Boden/Netzwerke/AGBoden/Downloads/KA5_bodenspezKennwerte.pdf?__blob=publicationFile&v=2) (last accessed 04 November 2024).
16. Geologischer Dienst Nordrhein-Westfalen 2024. Differenzierung der Bodenart [Differentiation of the soil type]. [https://www.gd.nrw.de/bo\\_korngroessenanalyse.htm](https://www.gd.nrw.de/bo_korngroessenanalyse.htm) (last accessed 04 November 2024).
17. Luong, T, Vorobevskii, I and Wiemann, S 2020. Pseudo-Spatially-Distributed Modeling of Walter Balance Components in the Free State of Saxony. *Hydrology*, **7**, 1-18.
18. Tóth, B, Weynants, M, Nemes, A, Makó, A, Bilas, G and Tóth, G 2015. New generation of hydraulic pedotransfer functions for Europe. *European Journal of Soil Science*, **66**, 226-238.
19. Geologischer Dienst Nordrhein-Westfalen 2024. Bodenkarte von Nordrhein-Westfalen 1:50000 – digital und analog [Soil map of North Rhine-Westphalia 1:50000 - digital and analogue]. [https://www.gd.nrw.de/pr\\_kd\\_bodenkarte-50000.php#bk50](https://www.gd.nrw.de/pr_kd_bodenkarte-50000.php#bk50) (last accessed 04 November 2024).
20. Landesanstalt für Umwelt Baden-Württemberg 2022. Bodenkarte (BK 50) [Soil map (BK 50)]. <https://rips-metadaten.lubw.de/trefferanzeige?docuuid=2ad74dd7-fe07-48a3-882f-aaac2403ce06> (last accessed 04 November 2024).